Sound & Vibration 2026, 60(1), 3669.
doi: https://doi.org/10.59400/sv3669

Article

Effect of stacking sequence and material properties on the damage detection of laminated composite plates using wavelet transform

Morteza Saadatmorad[1], Ramazan-Ali Jafari-Talookolaei[2,*], Hamidreza Ghandvar[3], Orifjon Mikhliev[4]

[1] Department of Civil, Chemical, Environmental and Materials Engineering, University of Bologna, Risorgimento Avenue 2, 40136 Bologna, Italy
[2] School of Mechanical Engineering, Babol Noshirvani University of Technology, Babol 47148-71167, Iran
[3] Department of Mechanical Engineering, School of Engineering, New Uzbekistan University, Tashkent 100007, Uzbekistan
[4] FIE UzLITI Engineering LLC, Tashkent 100099, Uzbekistan
*** Corresponding author:** Ramazan-Ali Jafari-Talookolaei, ramazanali@gmail.com or ra.jafari@nit.ac.ir

CITATION

Saadatmorad M, Jafari-Talookolaei RA, Ghandvar H, et al. Effect of stacking sequence and material properties on the damage detection of laminated composite plates using wavelet transform. Sound & Vibration. 2026; 60(1): 3669. https://doi.org/10.59400/sv3669

ARTICLE INFO

Received: 29 August 2025
Revised: 26 January 2026
Accepted: 30 January 2026
Available online: 9 February 2026

Abstract: Damage detection of laminated composite structures is crucial because damage may significantly compromise their structural integrity and lead to catastrophic failures. Traditional non-destructive testing (NDT) methods often prove inadequate for detecting subtle damage, such as delamination or matrix cracking, which can initiate and propagate within the composite material. Therefore, advanced damage detection techniques are essential to ensure the safety and reliability of these structures in various engineering applications. The wavelet transform is a popular non-destructive testing method for processing structural signals in laminated composites. According to the literature review, the effect of changes in laminated composite parameters on damage detection by wavelet transform is an open question. This research aims to investigate the effect of changing the parameters of laminated composite plates on the accuracy of damage detection by two-dimensional discrete wavelet transform (2D-DWT). In this paper, damaged rectangular laminated composite plates (RLCPs) are modeled to introduce damage detection by 2D-DWT and evaluate the effect of changes in RLCPs parameters. The considered parameters are the number of layers, composite material, strengths, size, and thickness of laminate composite layups. Various scenarios are tested, and findings show that among these parameters, the most influential parameter on damage detection of RLCPs by the two-dimensional discrete wavelet transform is the changes in material properties of RLCPs.

Keywords: damage detection; composite plates; wavelet transforms; laminated composite plates; stacking-up

1. Introduction

Composite structures are one of the ideal options for many engineering applications due to their characteristics such as high strength, low density, high modulus, excellent resistance to fatigue, etc. [1–3]. Due to their lightweight, composite structures are used in many high-speed applications, such as the body of racing cars and high-speed rail vehicles [4–6]. These applications cause them to be exposed to severe impacts and consequently to serve damages. For this reason, damage detection of composite structures is a necessity. Therefore, different researches have been conducted to detect and identify the damage on these structures [7].

Damage detection methods are usually non-destructive tests. The primary group of these methods is vibration-based damage detection methods because they use

vibration data to detect or identify damages in structures [8]. There are several major classes of vibration-based damage detection methods, such as Mode shape-based methods, optimization-based methods, Natural frequency-based methods, machine learning-based methods, wavelet-based methods, curvature/strain mode shape-based methods, and other methods based on modal parameters. Among these methods, wavelet-based methods are very suitable since they depend only on vibrational signals for detecting damages [9,10].

Most of the research has been conducted on wavelet transform to detect various isotropic structures; however, few studies have been performed on damage detection of rectangular laminated composite structures [11]. Saadatmorad et al. [12] investigated damage detection in marine laminated composite structures. They pointed out that the classical wavelet technique is less accurate in detecting low-level damage, and the noise in its results is problematic. This study presented a new method based on wavelet transform WT-RBFNs for accurate damage detection in marine fiberglass multilayer composite plates. In this research, a finite element model and a two-dimensional discrete wavelet transform were used to analyze vibration signals. Numerical and experimental results showed that the proposed method performed better than classical methods even for very low damage. Rucka and Wilde [13] used continuous wavelet transforms to detect damage in beams and plates. The material of the studied structures was isotropic. Katunin [14] developed a damage detection method for polymer composite plates using two-dimensional B-spline wavelets. His approach, validated through numerical results, employed finite element analysis to model the composite plate and a discrete wavelet transform algorithm with a sixth-order B-spline wavelet to analyze vibrational modes. Damage was detected based on the detail coefficient singular points, demonstrating the method's effectiveness for structural health monitoring. Chang and Chen [15] studied damage detection in rectangular steel plates using the spatial wavelet method. Katunin [16] studied tone impact damage identification in composite plates using modal data and quincunx wavelet analysis. This paper develops general-order two-dimensional B-spline wavelets and presents a discrete a wavelet transform algorithm. The vibration modes of a fixed laminated composite plate were modeled and analyzed. A damage identification method, based on wavelet detail coefficients, was then applied. Numerical results, experimentally verified, demonstrated the method's effectiveness in identifying damage. Azuara et al. [17] used a two-dimensional convolutional neural network and wavelet transform to localize damages in thermoplastic composite plates. This paper presented a convolutional neural network (CNN) that predicted distance-to-damage by analyzing transducer signals. The CNN used a 2D time-frequency image, generated from experimental signals via the Wavelet transform, as input. These distance predictions were then incorporated into a damage location algorithm, yielding a 2D surface image estimating damage location with 15 mm accuracy. Yan and Yam [18] investigated delamination detection in rectangular laminated composite plates based on modal strain energy. This paper investigated the detection of small, localized delamination in laminated composite plates using embedded piezoelectric patches. The method employed wavelet packet analysis to decompose structural dynamic

responses into various frequency bands, analyzing the energy distribution of structural vibration sub-signals. This in-situ approach, utilizing a limited number of embedded piezoelectric patch sensors and actuators, demonstrated higher sensitivity compared to existing methods. Results indicated the ability to detect delamination areas as small as 0.13% of the total composite plate area, with good agreement between numerical simulation and experimental results. Yang and Oyadiji [19] applied 2D-wavelet transforms for detecting damages in composite plates. This paper introduced a damage detection method using the modal frequency surface (MFS). The MFS was generated by attaching a point mass at varying locations. Delamination-induced local stiffness reduction caused discontinuities in the MFS. Finite element analysis showed that frequency deviations decreased quasi-exponentially with delamination depth. The magnitude of the MFS wavelet coefficient was then analyzed across various noise levels. Results demonstrated that the MFS wavelet coefficient effectively identifies the location and shape of both near-surface and far-surface delaminations in laminated composite plates. Sohn et al. [20] proposed a wavelet-based signal processing method for detecting delamination. This paper presented a wavelet-based signal processing technique for near-real-time delamination detection in composite structures. The technique integrated an active sensing system using piezoelectric patches to generate wavelet-form input signals and measure corresponding response signals. Wavelet transform analysis of the response signals extracted damage-sensitive features. Experimental results on a composite plate under varying temperature and boundary conditions demonstrated the method's effectiveness in identifying delamination. Cao and Qiao [21] proposed a new technique named "integrated wavelet transforms (IWTs)" for identifying damages in laminated composite beams. The technique mixed continuous wavelet transform (CWT), and stationary wavelet transform (SWT). Some other recent investigations on new versions and application is Wang et al., Jiang et al., He et al., and Saadatmorad et al. [22–26].

Based on the literature review, the effect of changes in laminated composite parameters on damage detection by wavelet transform is an open question, and this is a research gap. In this paper, damaged rectangular laminated composite plates are modeled to introduce damage detection by two-dimensional discrete wavelet transforms and evaluate the effect of changes in rectangular laminated composite parameters.

2. Materials and methods

Figure 1 shows the single-damaged RLCP considered in this study. The first-order shear deformation theory (FSDT) is used to introduce displacement fields of the considered RLCP. This RLCP has length a, thickness h, and width b, as shown in **Figure 1**.

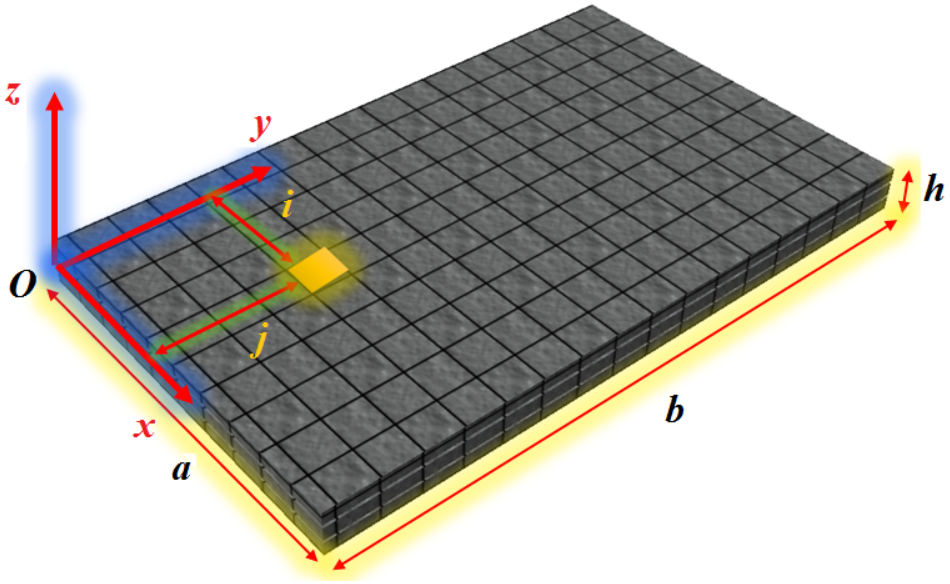

Figure 1. Model of the studied single-damaged RLCP.

Displacement fields of the considered RLCP based on the FSDT are formulated as follows [27]:

$$\begin{aligned} u(x,y,z,t) &= u_0(x,y,t) + z\,\psi_x(x,y,t) \\ v(x,y,z,t) &= v_0(x,y,t) + z\,\psi_y(x,y,t) \\ w(x,y,z,t) &= w_0(x,y,t) \end{aligned} \tag{1}$$

Where u, v and w are displacement functions in *x*-, *y*- and *z*-directions, respectively. Additionally, u_0, v_0 and w_0 ar the displacements at the mid-plane of the RLCP in the directions of *x*-, *y*- and *z*-, respectively. In addition, ψ_x and ψ_y show rotations about *y*- and x-directions, respectively.

Based on Equation (1) and by differentiation, the strain components can be obtained as:

$$\begin{aligned} &\varepsilon_x^0 = u_{0,x}, \quad &&\varepsilon_y^0 = v_{0,y}, \quad &&\gamma_{xy}^0 = u_{0,y} + v_{0,x} \\ &\kappa_x = \psi_{x,x}, \quad &&\kappa_y = \psi_{y,y}, \quad &&\kappa_{xy} = \psi_{x,y} + \psi_{y,x} \end{aligned} \tag{2}$$

In the above relations and the following equations, the symbol comma (,), symbolizes differentiation, concerning the variable after that. Based on the FSDT, the constitutive equations related to the RLCP are formulated as follows [28]:

$$\begin{Bmatrix} N_x \\ N_y \\ N_{xy} \\ M_x \\ M_y \\ M_{xy} \end{Bmatrix} = \begin{bmatrix} A_{11} & A_{12} & A_{16} & B_{11} & B_{12} & B_{16} \\ A_{12} & A_{22} & A_{26} & B_{12} & B_{22} & B_{26} \\ A_{16} & A_{26} & A_{66} & B_{16} & B_{26} & B_{66} \\ B_{11} & B_{12} & B_{16} & D_{11} & D_{12} & D_{16} \\ B_{12} & B_{22} & B_{26} & D_{12} & D_{22} & D_{26} \\ B_{16} & B_{26} & B_{66} & D_{16} & D_{26} & D_{66} \end{bmatrix} \begin{Bmatrix} \varepsilon_x^0 \\ \varepsilon_y^0 \\ \gamma_{xy}^0 \\ \kappa_x \\ \kappa_y \\ \kappa_{xy} \end{Bmatrix} \tag{4}$$

Where N_x, N_y, and N_{xy} are the resultant forces at the in-plane, M_x and M_y represent the bending moments, M_{xy} shows the twisting moment, Q_{yz} and Q_{xz} indicate the resultant shear forces. Also, A_{ij},B_{ij}, and $D_{ij}(i,j = 1,\ 2, \ldots,\ 6)$ are the extension,

bending–extension coupling, and bending stiffness, respectively, A_{ij} $(i,j=4,5)$ are the transverse shear stiffness. The above-mentioned quantities can be expressed as [29]:

$$A_{ij}=\sum_{k=1}^{N}\left(\overline{Q}_{ij}\right)_k\left(z_k-z_{k-1}\right)\qquad i,j=1,2,6 \tag{5}$$

$$B_{ij}=\frac{1}{2}\sum_{k=1}^{N}\left(\overline{Q}_{ij}\right)_k\left(z_k^2-z_{k-1}^2\right)\qquad i,j=1,2,6 \tag{6}$$

$$D_{ij}=\frac{1}{3}\sum_{k=1}^{N}\left(\overline{Q}_{ij}\right)_k\left(z_k^3-z_{k-1}^3\right)\qquad i,j=1,2,6 \tag{7}$$

$$A_{ij}=k_{ij}\sum_{k=1}^{N}\left(\overline{Q}_{ij}\right)_k\left(z_k-z_{k-1}\right)\quad i,j=45 \tag{8}$$

Where N is the number of layers of the RLCP, $\left(\overline{Q}_{ij}\right)_k$ is the transformed stiffness coefficients in the kth layer, z_k and z_{k-1} are distances from the top and bottom surfaces to the k^{th} layer from the plate's mid-plane, respectively, and k_{ij} are the shear correction factors.

The potential energy of the RLCP can be expressed as:

$$U_P=\frac{1}{2}\int_0^a\int_0^b\left(N_x\varepsilon_x^0+N_y\varepsilon_y^0+N_{xy}\gamma_{xy}^0+M_x\kappa_x+M_y\kappa_y+M_{xy}\kappa_{xy}+Q_{yz}\gamma_{yz}+Q_{xz}\gamma_{xz}\right)dy\,dx \tag{9}$$

By inserting Equations (2)–(4) into Equation (9), the potential energy can be obtained as:

$$\begin{aligned}U_P=&\tfrac{1}{2}\int_0^a\int_0^b\left[A_{11}u_{0,x}^2+A_{22}v_{0,y}^2+A_{66}\left(u_{0,y}^2+v_{0,x}^2+2u_{0,y}v_{0,x}\right)+D_{11}\psi_{x,x}^2+D_{22}\psi_{y,y}^2\right.\\&+D_{66}\left(\psi_{x,y}^2+\psi_{y,x}^2+2\psi_{x,y}\psi_{y,x}\right)+A_{44}\left(\psi_y^2+w_{0,y}^2+2\psi_y w_{0,y}\right)+A_{55}\left(\psi_x^2+w_{0,x}^2+2\psi_x w_{0,x}\right)\\&+2A_{12}u_{0,x}v_{0,y}+2A_{16}\left(u_{0,y}+v_{0,x}\right)u_{0,x}+2B_{11}\psi_{x,x}u_{0,x}+2B_{12}\psi_{y,y}u_{0,x}+2B_{16}\left(\psi_{x,y}+\psi_{y,x}\right)u_{0,x}\\&+2A_{26}\left(u_{0,y}+v_{0,x}\right)v_{0,y}+2B_{12}\psi_{x,x}v_{0,y}+2B_{22}\psi_{y,y}v_{0,y}+2B_{26}\left(\psi_{x,y}+\psi_{y,x}\right)v_{0,y}+2B_{16}\psi_{x,x}\left(u_{0,y}+v_{0,x}\right)\\&+2B_{26}\psi_{y,y}\left(u_{0,y}+v_{0,x}\right)+2B_{66}\left(\psi_{x,y}+\psi_{y,x}\right)\left(u_{0,y}+v_{0,x}\right)+2D_{12}\psi_{y,y}\psi_{x,x}+2D_{16}\left(\psi_{x,y}+\psi_{y,x}\right)\varnothing_{,x}\\&\left.+2D_{26}\left(\psi_{x,y}+\psi_{y,x}\right)\psi_{y,y}+2A_{45}(\psi_x+w_{0,x})(\psi_y+w_{0,y})\right]dydx\end{aligned} \tag{10}$$

The kinetic energy formulation for the considered RLCP is obtained as follows:

$$T=\frac{1}{2}\int_0^a\int_0^b\left[I_0\left(u_{,t}^2+v_{,t}^2+w_{,t}^2\right)+2I_1u_{,t}\psi_{x,t}+v_{,t}\psi_{y,t}+I_2\psi_{x,t}^2+\psi_{y,t}^2)\right]dy\,dx \tag{11}$$

Where $(I_0,\ I_1,\ I_2)$ show the mass moment of inertia obtained based on the bellow expression:

$$(I_0,\ I_1,\ I_2)=\int_{-h/2}^{h/2}\rho(z)\left(1,z,z^2\right)dz \tag{12}$$

3. Governing equations of motion

The global matrix of stiffness $[K]$ and the global matrix of mass $[M]$ can be obtained through assembling the local matrix of stiffness and the local matrix of mass, respectively. In order to implement the elastic boundary conditions, the elastic coefficients can be entered into the corresponding principal diagonal arrays within the global stiffness matrix. Next, the relations of motion related to the whole free vibrating

system can be formulated as [29]:

$$[M]\left\{\ddot{\Delta}\right\}+[K]\{\Delta\}=\{0\} \tag{13}$$

Where $\{\Delta\}$ encompasses the degrees of freedom for the total number of nodes of the presented FE model. In addition, by considering $\{\Delta\}=\{\Delta_0\}\,e^{i\omega t}$ and $\lambda=\omega^2$, the relation (13) is rewritten as:

$$([K]-\lambda[M])\,\{\Delta_0\}=0 \tag{14}$$

Where $\{\Delta_0\}$ contains the mode shapes vectors of the studied RLCP and ω shows the corresponding natural frequencies. The non-zero solution of Equation (14) can be obtained through solving $\det([K]-\lambda[M])=0$. This procedure leads to the mode shapes and their corresponding natural frequencies. The mentioned procedure is programmed and implemented employing MATLAB software.

Entering single-damage into the FE model

In this investigation, the single damages are applied to the FE model before assembling them in the global stiffness matrix via multiplying a given number called α as a damage index by local stiffness matrix ($[Ke]$) in FEM Matlab code for every single damage scenario [30]:

$$[Ke]_d=\alpha[Ke] \tag{15}$$

Where $[Ke]_d$ denotes the local stiffness matrix of a typical damaged element of the RLCP.

By employing the one-dimensional discrete wavelet transformation (1D-DWT), it is possible to decompose a given 1D-signal *f(x)* into an approximation signal plus detail signals as [31]:

$$f(x)=A_j(x)+\sum\nolimits_{j<J}D_j(x) \tag{16}$$

Where j is the level related to the wavelet decomposition.

The approximation signals related to the level *j* are expressed as:

$$A_j(x)=\sum\nolimits_{k=-\infty}^{+\infty}cA_{j,k}\phi_{j,k}(x) \tag{17}$$

Where $cA_{j,k}$ It shows coefficients related to the approximation signal at the level *j*. In addition, $\phi_{j,k}(x)$ denote the scaling function at the level *j*.

The detail sub-signals related to the level *j* are expressed as:

$$D_j(x)=\sum\nolimits_{k\epsilon Z}cD_{j,k}\psi_{j,k}(x) \tag{18}$$

Where $cD_{j,k}$ are coefficients of detail signal at the level *j*. Besides, $\psi_{j,k}(x)$ is called wavelet function.

In wavelet transformations, the vanishing moment is the most significant determinant affecting the identification of damages or faults in signals. When a

wavelet transform has *n* vanishing moments, the following equation has to be satisfied:

$$\int_{-\infty}^{+\infty} x^i \psi(x) dx = 0,\ i = 1, 2, \ldots,\ n - 1\text{b}) \tag{19}$$

The one-dimensional scaling and wavelet functions can be extended as two-dimensional scaling and wavelet functions because the 2D-wavelet transformation may be presented in the form of tensor products concerning the 1D-wavelet transformation as [32]:

$$\begin{aligned} \phi(x,y) &= \phi(x)\phi(y) \\ \psi^H(x,y) &= \phi(x)\psi(y) \\ \psi^V(x,y) &= \psi(x)\phi(y) \\ \psi^D(x,y) &= \psi(x)\psi(y) \end{aligned} \tag{20}$$

where $\phi(x,y)$ is the scaling function. $\psi^H(x,y)$, $\psi^V(x,y)$, and $\psi^D(x,y)$ are the wavelet transformation functions applied in horizontal, vertical, and diagonal directions, respectively [32].

Therefore, the 2D-signal *f(x,y)* or the image may be decomposed into four various quarter-sized images (i.e., W_ϕ as an approximation sub-image, and W_ψ^H, W_ψ^V, W_ψ^D as detail sub-images in horizontal, vertical, and diagonal directions, respectively) at level *j*.

In this paper, single-level 2D-DWTs decompose the 2D vibration amplitude signals related to the studied damaged RLCP. Also, the diagonal detail signal is used as the damage index because, according to the literature, the diagonal detail signal is considered the most effective for identifying point damages (damages that do not extend in horizontal or vertical directions).

Assuming the size of $I(i,q)$ is $n \times m$, the following relation is related to the diagonal detail signal obtained from the two-dimensional discrete wavelet transform:

$${D^D}_{j,m,n}(i,q) = \frac{1}{2} \sum_{i=0}^{m-1} \sum_{q=0}^{n-1} I(i,q) 2^{\frac{-j}{2}} \psi^D(2^{-j}i - m,\ 2^{-j}q - n) \tag{21}$$

where $I(i,q)$ is the original two-dimensional signal (i.e., mode shape), ${D^D}_{j,m,n}(i,q)$ denotes the diagonal detail signal.

4. Results

In general, the effects of changes in the parameters of the laminated composite can be investigated from two aspects: the effect of parameters on the vibration signals, and the effect of parameters on outputs of wavelet transforms. Here, both aspects are investigated. Note that the sensitivity of wavelet-based approaches to damage is generally higher in higher-order modes. Thus, in this study, we used the fourth mode shape. Also, the wavelet transform is inherently weak in detecting damage at the edges of the structure; therefore, in the damage scenarios, no damage at the boundary of the structure is considered.

4.1. Effects of lay-ups and number of layers

In this section, numerical investigations on the effects of lay-ups and the number of layers on damage detection of RLCP are presented. First, a general finite element program is developed to cover the vibration analysis of RLCPs with the different numbers of layers and stacking-ups and generate the corresponding vibration amplitude signals. A nine-node rectangular element in each node with five degrees of freedom is used to mesh the RLCPs. As seen in **Figure 2** and **Table 1**, the studied RLCPs are divided into 15 × 15 finite elements. It is assumed that actual single damage exists at location $(i, j) = (5,5)$, and damage severity is 50%.

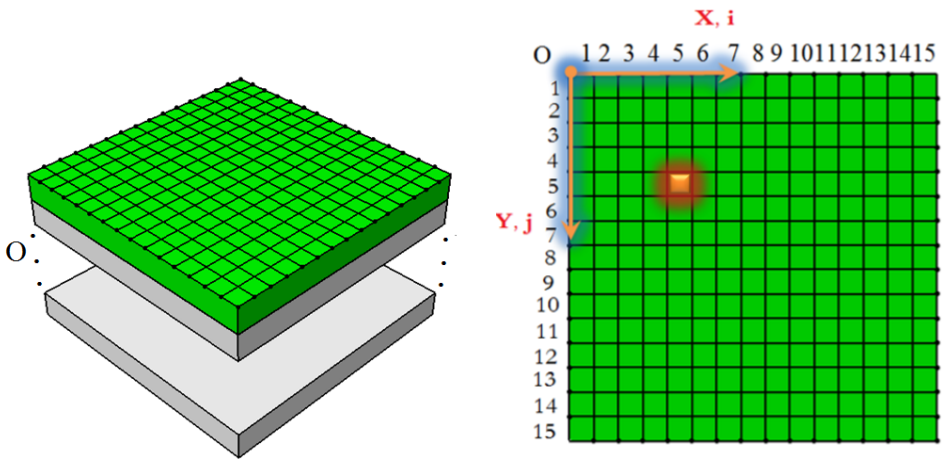

(a) **(b)**

Figure 2. **(a)** 3D view of RLCPs divided as 15 × 15 finite elements; **(b)** Top view of RLCPs divided as 15 × 15 finite elements with damage location studied in the current research (with the level of 50%).

Table 1. Damage scenarios in the current numerical investigation.

Scenario	Damage location		Damage severity	Number of layers
	i	***j***	**50%**	
S1	5	5	50%	2
S2	5	5	50%	3
S3	5	5	50%	4
S4	5	5	50%	6

After trial-and-error simulations, it is found that the Symlet wavelet function with vanishing moments 4 is the best mother wavelet function for this numerical investigation. Note that while different wavelet functions can yield varying responses, we maintained a constant wavelet function to isolate the effects of geometric, dimensional, and material parameters on damage detection in our parametric study. Also, wavelet transforms are applied at level 1 in all scenarios.

Figure 3 shows laminated composites' parameters for scenarios 1 and 2. **Figure 4** indicates laminated composites' parameters for scenarios 3 and 4.

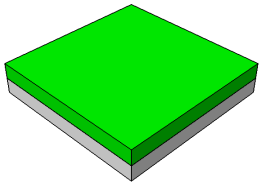

Case 1: Lay-up 1: [0°/45°]
Case 2: Lay-up 2: [90°/0°]

(a) Scenario 1 (S1).

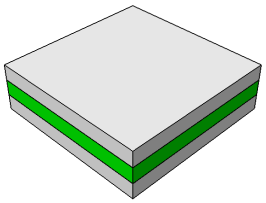

Case 1: Lay-up 1: [0°/90°/0°]
Case 2: Lay-up 2: [90°/0°/90°]

(b) Scenario 2 (S2).

Figure 3. Laminated composites' parameters for scenarios 1 and 2.

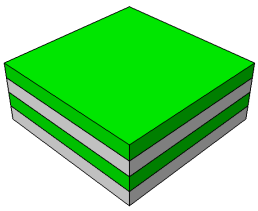

Case 1: Lay-up 1: [0°/90°/90°/0°]
Case 2: Lay-up 2: [0°/30°/60°/0°]

(a) Scenario 1 (S1).

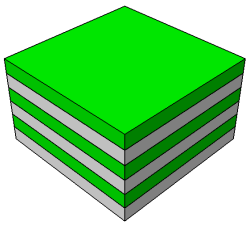

Case 1: Lay-up 1: [−45°/45°/−45°/45°/−45°/45°]
Case 2: Lay-up 2: [45°/−45°/45°/−45°/45°/−45°]

(b) Scenario 4 (S4).

Figure 4. Laminated composites' parameters for scenarios 3 and 4.

Table 2 shows characteristics of the studied finite element model of the RLCPs for evaluating the effects of lay-ups and the number of layers.

Table 2. Characteristics of the studied finite element model of the RLCPs.

Parameter	Description or value
a	0.2 m
b	0.2 m
h	$0.1a$
Dividing elements	15×15
Shear Factor	$k_s = 5/6$
Young's modulus	$E_{22} = 9.65$ GPa, $E_{11} = 25 \times E_{22}$
Shear modulus	$G_{12} = G_{13} = 0.5, E_{22}G_{13} = 0.2E_{22}$
Poisson's ratios	$\nu_{12} = 0.25, \nu_{21} = \frac{E_{22}}{E_{11}}\nu_{12}$

Scenario 1

In scenario 1, damage detection is performed for two different two-layer RLCPs. The first is related to an RLCP with lay-up [0°/45°] and then with the lay-up [90°/0°].

Scenario 2

In scenario 2, damage detection is done for two different two-layer RLCPs. The first is related to an RLCP with lay-up [0°/90°/0°] and then with the lay-up [90°/0°/90°].

Figure 5: (a) Contour plot of damaged signal of scenario 2 for Lay-up 1, (b) contour plot of damaged signal of scenario 2 for Lay-up 2, (c) plot of wavelet coefficient of scenario 2 for Lay-up 1 at level 1, (d) plot of wavelet coefficient of scenario 2 for Lay-up 2 at level 1.

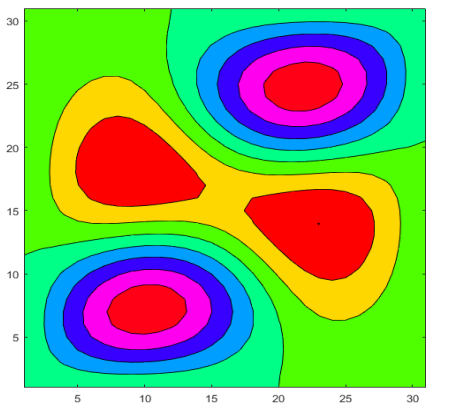

Scenario 1, case 1.

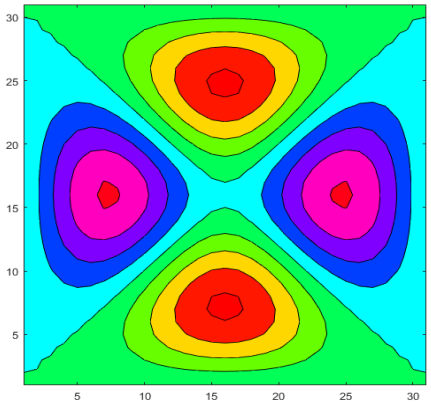

Scenario 1, case 2.

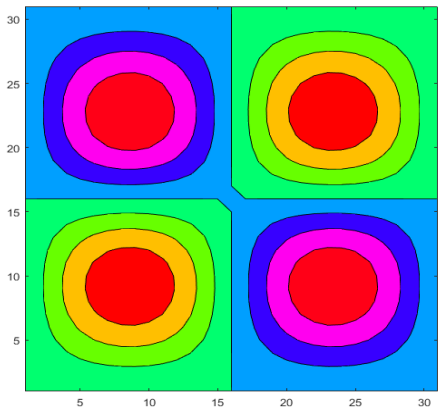

Scenario 2, case 1.

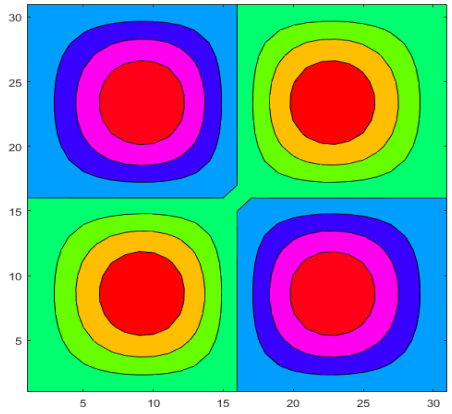

Scenario 2, case 2.

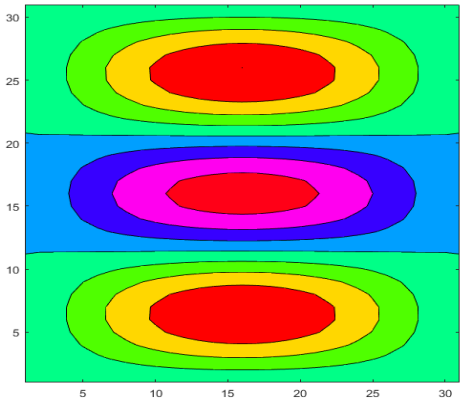

Scenario 3, case 1.

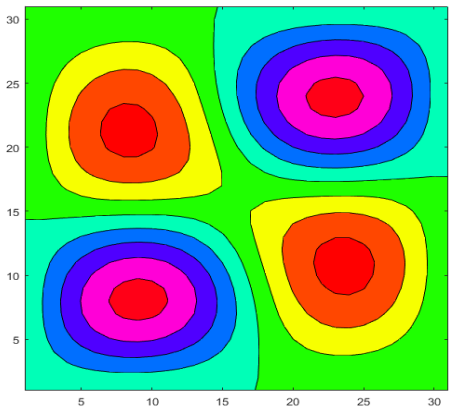

Scenario 3, case 2.

Figure 5. *Cont.*

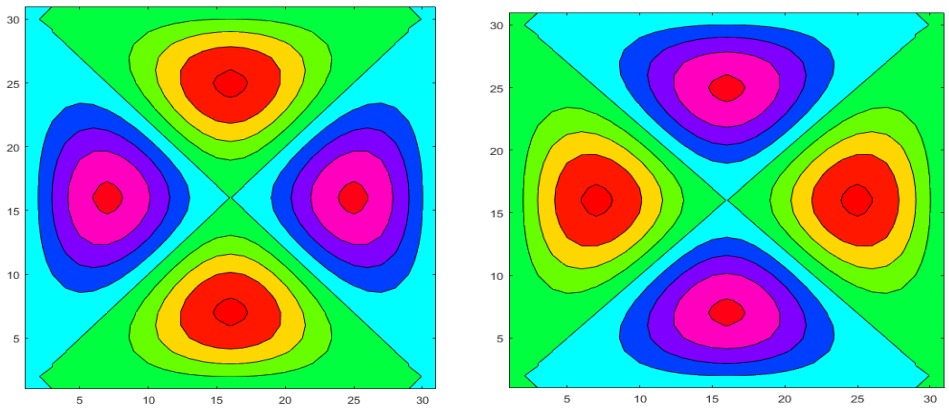

Scenario 4, case 1. Scenario 4, case 2.

Figure 5. Signals obtained from the developed FE model for intact rectangular laminated plates are described in four scenarios.

Scenario 3

In scenario 3, damage detection is done for two different two-layer RLCPs. The first is related to an RLCP with lay-up [0°/90°/90°/0°] and then with the lay-up [0°/30°/60°/0°].

Figure 5: (a) Contour plot of damaged signal of scenario 3 for Lay-up 1, (b) contour plot of damaged signal of scenario 3 for Lay-up 2, (c) plot of wavelet coefficient of scenario 3 for Lay-up 1 at level 1, (d) plot of wavelet coefficient of scenario 3 for Lay-up 2 at level 1.

Scenario 4

In scenario 4, damage detection is done for two different two-layer RLCPs. The first is related to an RLCP with lay-up [−45°/45°/−45°/45°/−45°/45°] and then with the lay-up [45°/−45°/45°/−45°/45°/−45°].

Figure 6 demonstrates signals obtained from the developed FE model for intact rectangular laminated intact plates described in four scenarios. **Figure 7** demonstrates signals obtained from the developed FE model for damaged rectangular laminated intact plates described in four scenarios.

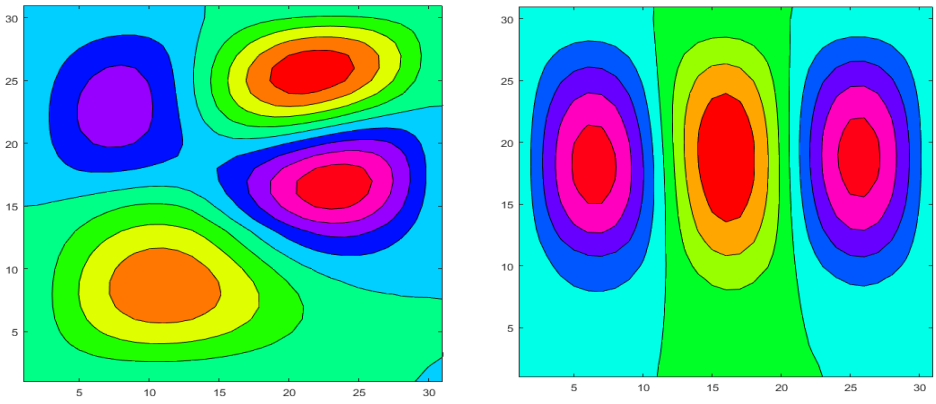

Scenario 1, case 1. Scenario 1, case 2.

Figure 6. *Cont.*

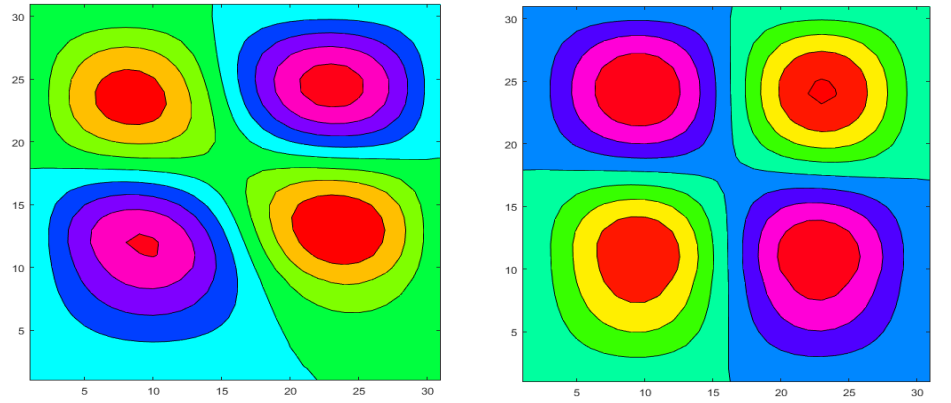

Scenario 2, case 1. Scenario 2, case 2.

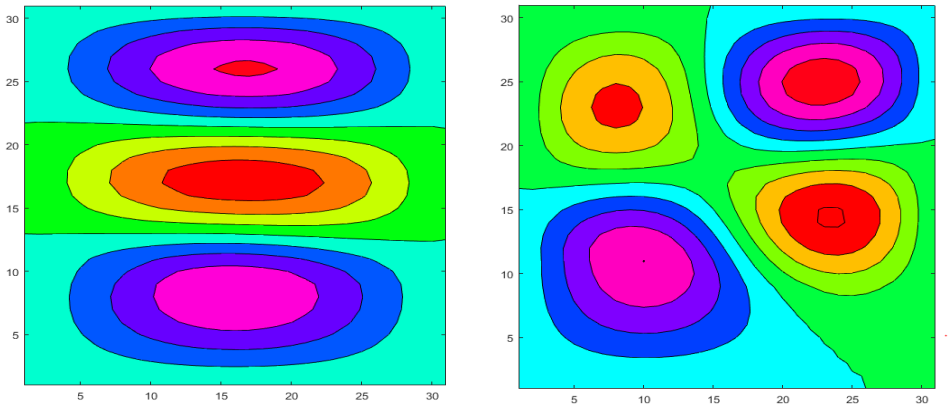

Scenario 3, case 1. Scenario 3, case 2.

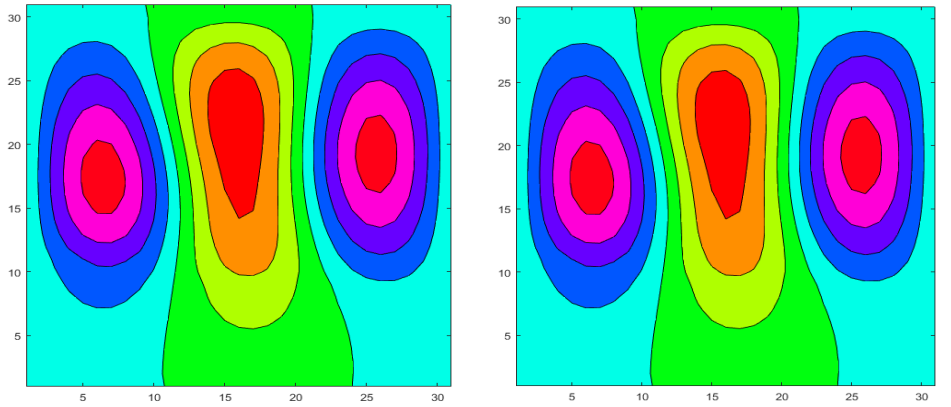

Scenario 4, case 1. Scenario 4, case 2.

Figure 6. Signals obtained from the developed FE model for damaged rectangular laminated intact plates described two scenarios in **Figure 5**.

As seen in **Figure 6**, when the rectangular laminated composite plates are intact, the geometry of their form signals is entirely symmetric in all scenarios and cases. Also, **Figure 6** shows that when the rectangular laminated composite plates are damaged, there are no symmetric signals in all scenarios and cases. In other words, asymmetry in the geometric shape of the signal indicates the structure is damaged.

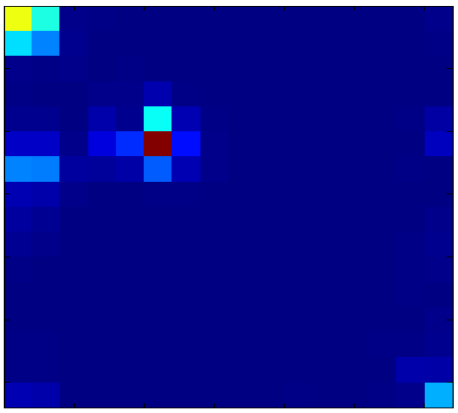

Scenario 1, case 1.

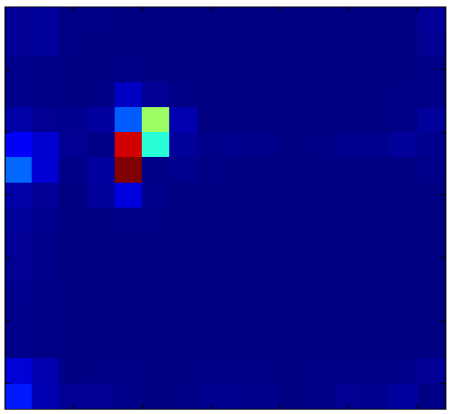

Scenario 1, case 2.

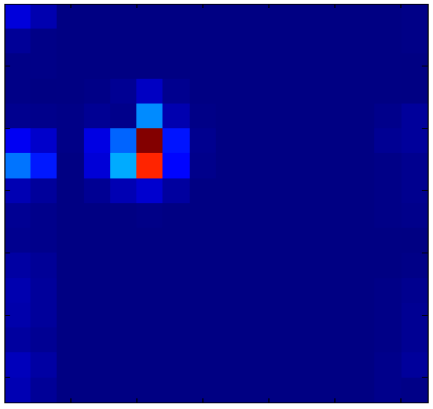

Scenario 2, case 1.

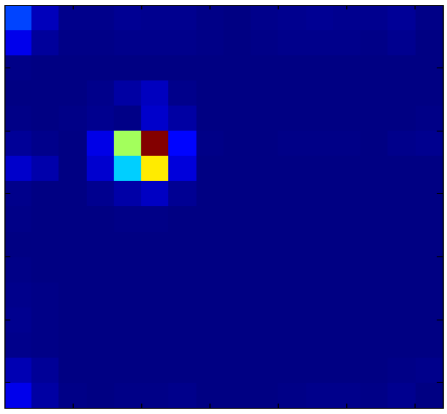

Scenario 2, case 2.

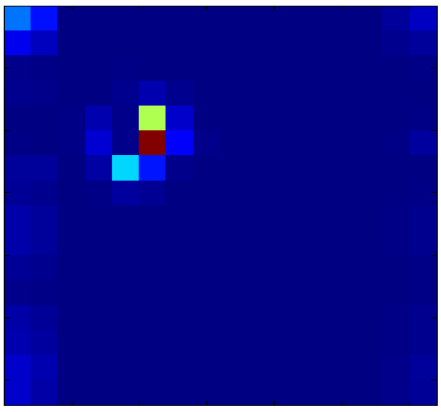

Scenario 3, case 1.

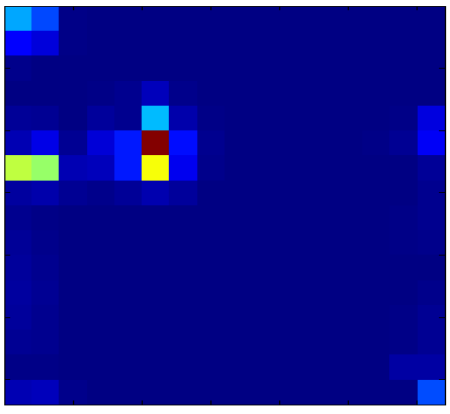

Scenario 3, case 2.

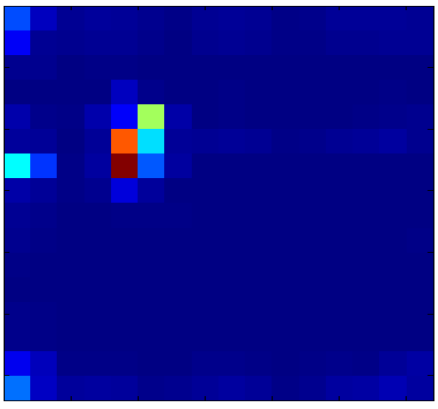

Scenario 4, case 1.

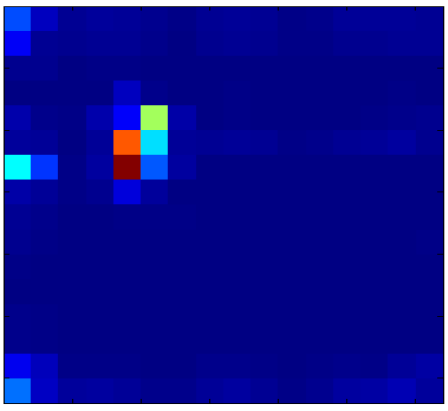

Scenario 4, case 2.

Figure 7. Results of damage detection by 2D-DWT for four damage scenarios.

According to **Figure 7**, it is found that a change in lay-ups in a given number of layers in RLCPs sometimes changes the detected location of damage, but very slightly, partially, and not significantly. In scenario 4, for the six-layer RLCP with lay-ups [−45°/45°/−45°/45°/−45°/45°] and [45°/−45°/45°/−45°/45°/−45°], damaged signals and wavelet coefficients are the same. According to **Figures 6** and **7**, as the number of layers of RLCPs increases or changes, the damaged signals change; as a result, wavelet coefficients change. Also, an increase in the number of layers of RLCPs has no negative or positive effect on the accuracy of damage detection.

4.2. Effects of changes in material properties

In this section, numerical investigations on the effects of changes in material properties on damage detection of RLCP are presented. It is assumed that the single damage is located at the position $(i, j) = (5, 5)$, and the level of damage is 70%. **Figure 8** shows the laminated composites' parameters in two scenarios for investigating the effects of changes in material properties on damage detection of RLCPs.

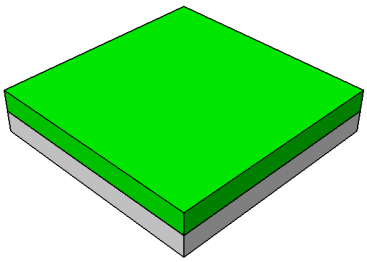

Scenario 1: [0°/45°]

Parameter	Description or value
a	0.2
b	0.2
h	$0.2a$
Dividing elements	15×15
Shear Factor	$k_s = 5/6$
Young's modulus	$E_{22} = 8$ GPa $\quad E_{11} = 30 \times E_{22}$
Shear modulus	$G_{12} = G_{13} = 0.6E_{22}, G_{23} = 0.3E_{22}$
Poisson's ratios	$\nu_{12} = 0.24, \nu_{21} = \frac{E_{22}}{E_{11}}\nu_{12}$

(a) Scenario 1 (S1).

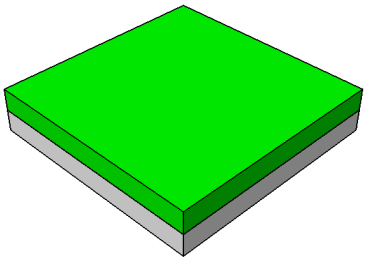

Scenario 2: [0°/45°]

Parameter	Description or value
a	0.2
b	0.2
h	$0.2a$
Dividing elements	15×15
Shear Factor	$k_s = 5/6$
Young's modulus	$E_{22} = 7.20$ GPa, $\quad E_{11} = 20 \times E_{22}$
Shear modulus	$G_{12} = G_{13} = 0.5E_{22}, G_{23} = 0.2E_{22}$
Poisson's ratios	$\nu_{12} = 0.23, \nu_{21} = \frac{E_{22}}{E_{11}}\nu_{12}$

(b) Scenario 2 (S1).

Figure 8. Laminated composites' parameters in two scenarios for investigating the effects of changes in material properties on damage detection of RLCPs.

Figure 9 indicates signals obtained from the developed FE model for damaged rectangular laminated intact plates described two scenarios in **Figure 8**.

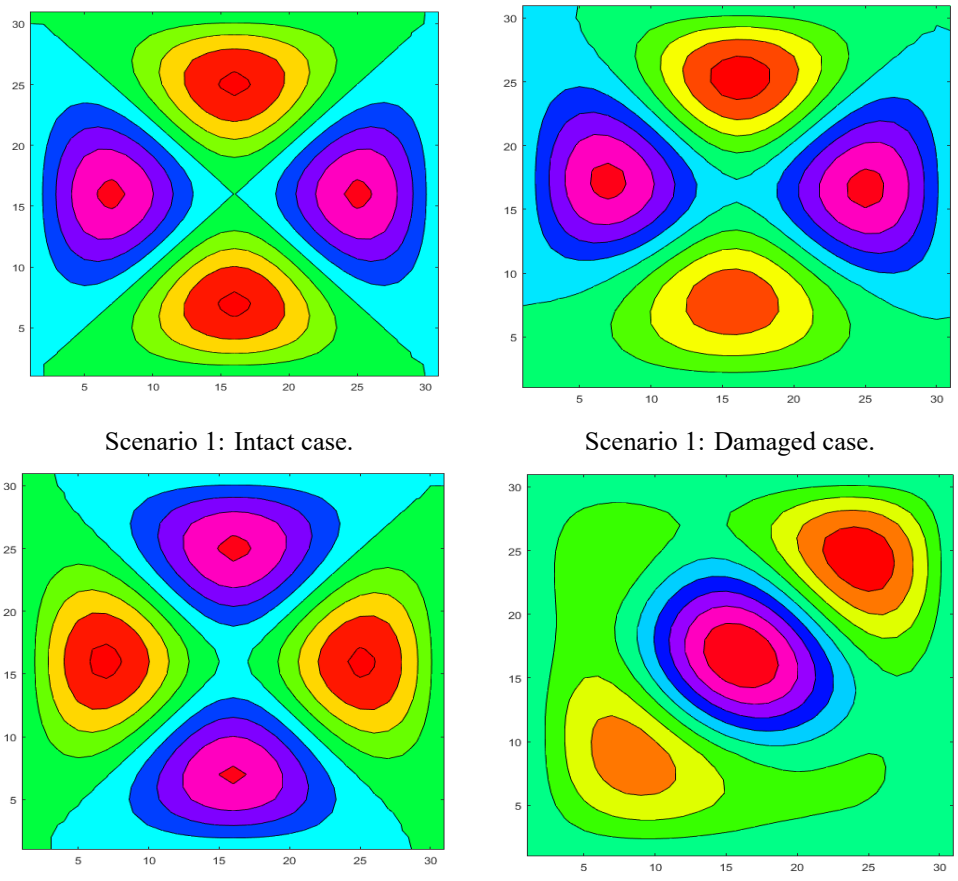

Scenario 1: Intact case. Scenario 1: Damaged case.

Scenario 2: Intact case. Scenario 2: Damaged case.

Figure 9. Signals obtained from the developed FE model for damaged rectangular laminated intact plates described two scenarios in **Figure 8**.

As seen in **Figure 9**, when the rectangular laminated composite plates are intact, the geometry of their form signals is entirely symmetric in all scenarios and cases. Also, **Figure 9** shows that when the rectangular laminated composite plates are damaged, there are no symmetric signals in all scenarios and cases. As mentioned, asymmetry in the geometric shape of the signal indicates the structure is damaged.

According to **Figure 10**, it is found that changes in material properties in RLCPs changes detected the location of damage significantly.

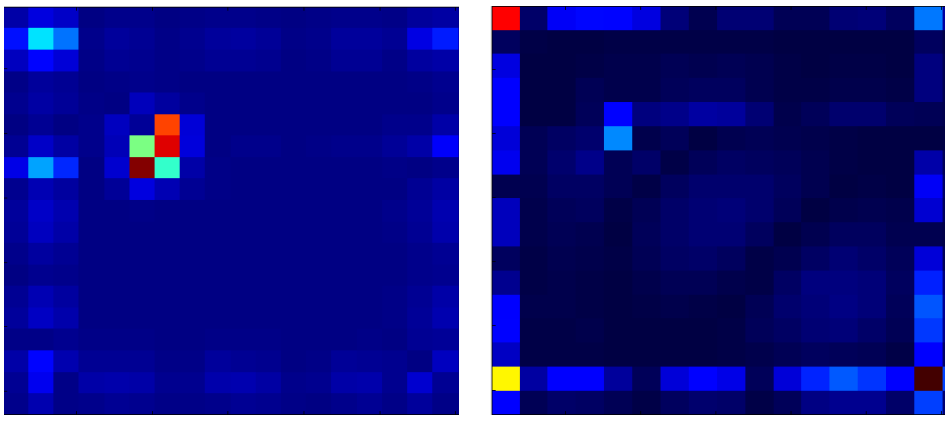

Scenario 1 Scenario 2

Figure 10. Results of damage detection by 2D-DWT for two damage scenarios for investigating the effects of changes in material properties on damage detection of RLCPs.

4.3. Effect size and thickness

In this section, numerical investigations on the effects of size and thickness on damage detection of RLCP are presented. It is assumed that the single damage is located at the position $(i, j) = (10, 8)$, and the level of damage is 70%. **Figure 11** shows the laminated composites' parameters in two scenarios for investigating the effects of changes in size and thickness on damage detection of RLCPs.

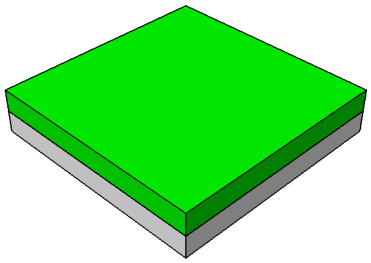

Scenario 1: Lay-up: [0°/45°]

Parameter	Description or value
a	0.9
b	0.9
h	$0.2a$
Dividing elements	15×15
Shear Factor	$k_s = 5/6$
Young's modulus	$E_{22} = 800 \times 10^7$, $E_{11} = 30 \times E_{22}$
Shear modulus	$G_{12} = G_{13} = 0.6E_{22}$, $G_{23} = 0.3E_{22}$
Poisson's ratios	$\nu_{12} = 0.24$, $\nu_{21} = \frac{E_{22}}{E_{11}}\nu_{12}$

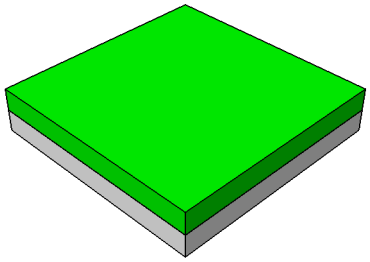

Scenario 2: Lay-up: [0°/45°]

Parameter	Description or value
a	0.2
b	0.2
h	$0.1a$
Dividing elements	15×15
Shear Factor	$k_s = 5/6$
Young's modulus	$E_{22} = 800 \times 10^7$, $E_{11} = 30 \times E_{22}$
Shear modulus	$G_{12} = G_{13} = 0.6E_{22}$, $G_{23} = 0.3E_{22}$
Poisson's ratios	$\nu_{12} = 0.24$, $\nu_{21} = \frac{E_{22}}{E_{11}}\nu_{12}$

Figure 11. Laminated composites' parameters in two scenarios for investigating the effects of changes in size and thickness on damage detection of RLCPs.

Figure 12 shows damaged signals and damage locations detected by 2D-WT for investigating the effects of size and thickness on damage detection of RLCPs.

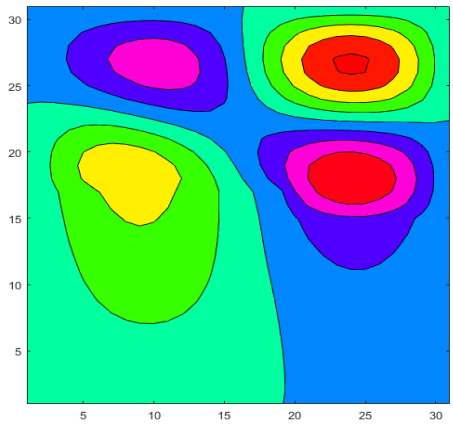

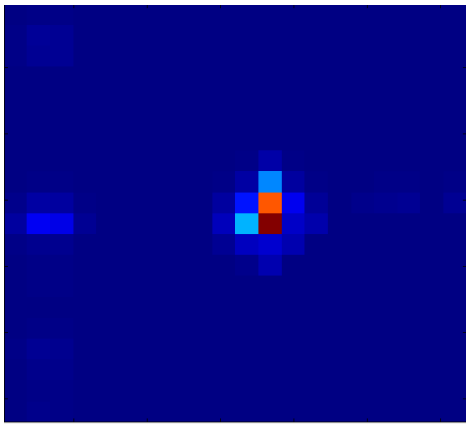

Damaged Signal. Damage location detected.

Scenario 1

Figure 12. *Cont.*

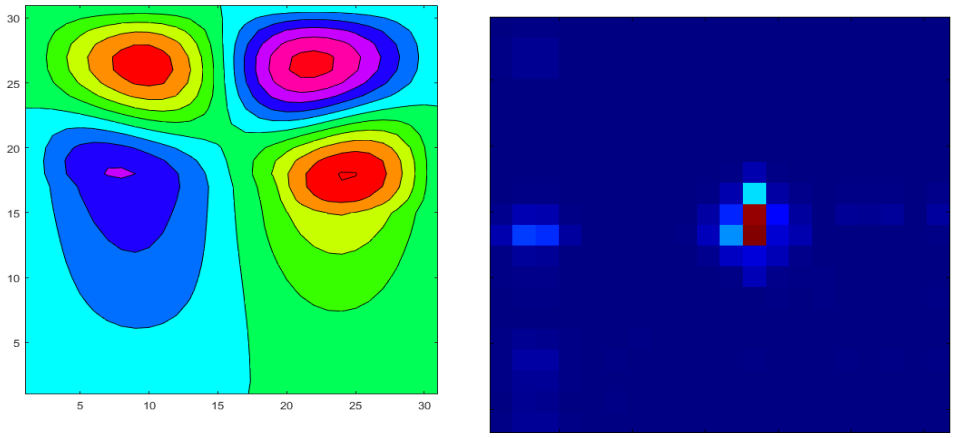

Damaged Signal. Damage location detected.

Scenario 2

Figure 12. Damaged signals and damage locations detected by 2D-WT for investigating the effects of size and thickness on damage detection of RLCPs.

As seen in **Figure 12**, change in size and thickness in RLCPs varies detected location of damage but very slightly, partially, and not significantly.

5. Conclusion

Damage detection using the wavelet transform method is proposed as one of the efficient methods. Several researches have been conducted to identify damage using the wavelet transform method in the laminated composite plate. On the other hand, different properties and parameters of composite laminate sheets significantly affect their performance and behavior. Among these studies, no research has investigated the effects of changes in the various properties of the laminate composite plate on the accuracy of damage detection. The purpose of this study is to fill this research gap. Note that noise can significantly affect the wavelet coefficients and the damage localization results. However, we needed an equal condition to examine the effect of the parameters. Due to the random nature of noise, the presence of random noise could have had a side effect in tracking the magnitude of the effects of different parameters.

Based on the findings of the forthcoming research, the following conclusions are presented:

- When the rectangular laminated composite plates are intact, the geometry of their form signals is entirely symmetric in all scenarios and cases.
- Asymmetry in the geometric shape of the signal indicates the structure is damaged.
- It is found that change in lay-ups in a given number of layers in RLCPs sometimes changes the detected location of damage, but very small and partial and not significantly.
- As the number of layers of RLCPs increases or changes, the damaged signals change; as a result, wavelet coefficients change.
- An increase in the number of layers of RLCPs has no negative or positive effect on the accuracy of damage detection.
- It is found that changes in material properties in RLCPs changes detected the location of damage significantly.

- Change in size and thickness in RLCPs varies with the detected location of damage, but very slightly, partially, and not significantly.

This research was limited by its examination of single damage scenarios and the lack of noise consideration, which future studies should address.

Author contributions: MS: Conceptualization, methodology, software, validation, formal analysis, investigation, data curation, and writing—original draft preparation. RAJT: Conceptualization, methodology, software, validation, and writing—review and editing. HG: Conceptualization, project administration, and writing—review and editing. OM: Conceptualization, project administration, and writing—review and editing. All authors have read and agreed to the published version of the manuscript.

Funding: This work received no external funding.

Institutional review board statement: Not applicable.

Informed consent statement: Not applicable.

Data availability statement: The data used in this study are available from the corresponding author upon reasonable request.

Conflict of interest: The authors declare no conflict of interest.

References

1. Khanahmadi M, Mirzaei B, Amiri GG, et al. Vibration-based damage localization in 3D sandwich panels using an irregularity detection index (IDI) based on signal processing. Measurement. 2024; 224: 113902.
2. Khanahmadi M. An effective vibration-based feature extraction method for single and multiple damage localization in thin-walled plates using one-dimensional wavelet transform: A numerical and experimental study. Thin-Walled Structures. 2024; 204: 112288.
3. Katunin A. Vibration-based spatial damage identification in honeycomb-core sandwich composite structures using wavelet analysis. Composite Structures. 2014; 118: 385–391.
4. Le Thanh C, Nguyen TN, Vu TH, et al. A geometrically nonlinear size-dependent hypothesis for porous functionally graded micro-plate. Engineering with Computers. 2022; 38(Suppl 1): 449–460.
5. Saitta S, Luciano R, Vescovini R, et al. Free vibrations and buckling analysis of cross-ply composite nanoplates by means of a Mesh Free Radial Point Interpolation Method. Composite Structures. 2022; 298: 115989.
6. Marec A, Thomas JH, El Guerjouma R. Damage characterization of polymer-based composite materials: Multivariable analysis and wavelet transform for clustering acoustic emission data. Mechanical systems and signal processing. 2008; 22(6): 1441–1464.
7. Khatir S, Tiachacht S, Le Thanh C, et al. An improved artificial neural network using arithmetic optimization algorithm for damage assessment in FGM composite plates. Composite Structures. 2021; 273: 114287.
8. Khanahmadi M. A cutting-edge framework for damage-sensitive feature extraction leveraging modal dynamic flexibility in signal processing-driven structural health monitoring. Thin-Walled Structures. 2025; 216(Part A): 113617.
9. Qiao P, Lu K, Lestari W, et al. Curvature mode shape-based damage detection in composite laminated plates. Composite Structures. 2007; 80(3): 409–428.
10. Katunin A. The construction of high-order B-spline wavelets and their decomposition relations for fault detection and localisation in composite beams. Scientific Problems of Machines Operation and Maintenance. 2011; 46(3): 43–59.
11. Khatir S, Wahab MA, Boutchicha D, et al. Structural health monitoring using modal strain energy damage indicator coupled with teaching-learning-based optimization algorithm and isogeometric analysis. Journal of Sound and Vibration. 2019; 448: 230–246.
12. Saadatmorad M, Jafari-Talookolaei RA, Pashaei MH, et al. A robust technique for damage identification of marine

fiberglass rectangular composite plates using 2-D discrete wavelet transform and radial basis function networks. Ocean Engineering. 2022; 263: 112317.
13. Rucka M, Wilde K. Application of continuous wavelet transform in vibration based damage detection method for beams and plates. Journal of Sound and Vibration. 2006; 297(3–5): 536–550.
14. Katunin A. Damage identification in composite plates using two-dimensional B-spline wavelets. Mechanical Systems and Signal Processing. 2011; 25(8): 3153–3167.
15. Chang CC, Chen LW. Damage detection of a rectangular plate by spatial wavelet based approach. Applied Acoustics. 2004; 65(8): 819–832.
16. Katunin A. Stone impact damage identification in composite plates using modal data and quincunx wavelet analysis. Archives of Civil and Mechanical Engineering. 2015; 15(1): 251–261.
17. Azuara G, Ruiz M, Barrera E. Damage localization in composite plates using wavelet transform and 2-D convolutional neural networks. Sensors. 2021; 21(17): 5825.
18. Yan YJ, Yam LH. Detection of delamination damage in composite plates using energy spectrum of structural dynamic responses decomposed by wavelet analysis. Computers and Structures. 2004; 82(4–5): 347–358.
19. Yang C, Oyadiji SO. Delamination detection in composite laminate plates using 2D wavelet analysis of modal frequency surface. Computers and Structures. 2017; 179: 109–126.
20. Sohn H, Park G, Wait JR, et al. Wavelet-based active sensing for delamination detection in composite structures. Smart Materials and Structures. 2003; 13(1): 153.
21. Cao M, Qiao P. Damage detection of laminated composite beams with progressive wavelet transforms. In: Shull P (editor). Nondestructive Characterization for Composite Materials, Aerospace Engineering, Civil Infrastructure, and Homeland Security 2008: At SPIE Smart Structures and Materials + Nondestructive Evaluation and Health Monitoring. SPIE—International Society for Optics and Photonics; 2008; 6934.
22. Wang Y, Deng T, Huang J, et al. A noise-robust, baseline-free, and adaptive damage indicator of plate-like structures based on the multicomponent information separation of high-resolution mode shapes using wavelets. Sensors. 2025; 25(9): 2669.
23. Jiang X, Ma K, Wu J, et al. Bridge damage identification based on variational modal decomposition and continuous wavelet transform method. Applied Sciences. 2025; 15(12): 6682.
24. He M, Wang M, Wu D, et al. CFRP composite fatigue damage pattern recognition using ultrasonic guided waves. Composite Structures. 2025: 119459.
25. Saadatmorad M, Jafari-Talookolaei RA, Khatir S, et al. Continuous frugal wavelet transform for damage detection in frame structures. Applied Acoustics. 2025; 234: 110621.
26. Abdushkour HA, Saadatmorad M, Khatir S, et al. Structural damage detection by derivative-based wavelet transforms. Arabian Journal for Science and Engineering. 2024; 49(11): 15701–15709.
27. Liu B, Ferreira AJM, Xing YF, et al. Analysis of composite plates using a layerwise theory and a differential quadrature finite element method. Composite Structures. 2016; 156: 393–398.
28. Reddy JN. Mechanics of Laminated Composite Plates and Shells: Theory and Analysis, 2nd ed. CRC Press; 2003.
29. Chen Y, Shao Z, Peng X, et al. A modified non-partial derivative perturbation meshfree approach with second-order statistical moments for vibration of cylindrical composite plate with random fields using KL expansion. Mechanics Based Design of Structures and Machines. 2025: 1–37.
30. Tran-Ngoc H, Khatir S, Ho-Khac H, et al. Efficient artificial neural networks based on a hybrid metaheuristic optimization algorithm for damage detection in laminated composite structures. Composite Structures. 2021; 262: 113339.
31. Bagheri A, Ghodrati Amiri G, Khorasani M, et al. Structural damage identification of plates based on modal data using 2D discrete wavelet transform. Structural Engineering and Mechanics. 2011; 40(1): 13–28.
32. Mallat SG. A theory for multiresolution signal decomposition: The wavelet representation. IEEE Transactions on Pattern Analysis and Machine Intelligence. 1989; 11(7): 674–693.